ISSN 0029-3865

CBPF - CENTRO BRASILEIRO DE PESQUISAS FÍSICAS
Rio de Janeiro

Notas de Física CBPF-NF-010/20
December 2020

Partial alpha-decay half-life of ^{178}Hf^{m2} isomer

O.A.P. Tavares, E.L. Medeiros and M.L. Terranova

NIB Núcleo de Informação C&T e Biblioteca

MINISTÉRIO DA CIÊNCIA, TECNOLOGIA, INOVAÇÕES E COMUNICAÇÕES
PÁTRIA AMADA BRASIL GOVERNO FEDERAL

Partial alpha-decay half-life of ^{178}Hf^{m2} isomer*

O A P Tavares[a], E L Medeiros[a,†], and M L Terranova[b]

[a]Centro Brasileiro de Pesquisas Físicas - CBPF/MCTIC
Rua Dr. Xavier Sigaud 150, 22290-180 Rio de Janeiro-RJ, Brazil

[b]Dipartimento di Scienze e Tecnologie Chimiche
Università degli Studi di Roma "TorVergata"
via dela Ricerca Scientifica s/n, 00133 Roma, Italy

Abstract - A simple, semi-empirical, one-parameter calculation model based on the quantum mechanical tunneling mechanism through a potential barrier has been used to estimate the partial α-decay half-life, $T^{\alpha}_{1/2}$, of ^{178}Hf^{m2} isomer. Alpha-transitions to levels of the ground-state band $J^{\pi} = 0^{+}, 2^{+}, \ldots, 14^{+}$ of ^{174}Yb have been considered, and the contributions to $T^{\alpha}_{1/2}$ due to overlapping, Coulomb, and centrifugal barriers have been detailed in each case. Results have indicated a $T^{\alpha}_{1/2}$-value of (0.24 ± 0.07) Gyr and a predominance ($\sim 57\,\%$) of α-particles populating the level $J^{\pi} = 6^{+}$, $E_{\gamma} = 526$ keV, compatible with results by other authors. Besides, a single, universal-like formula to estimate half-life of alpha transitions, whatever ℓ-value and the characteristics of the parent nucleus (e-e, e-o, o-e, and o-o nuclei, whether in the ground or isomeric states), has been envisaged.

PACS: 21.10.-k, 23.60.+e, 27.70.+q

Key-words: Alpha decay; ^{178}Hf^{m2} isomer; Half-life determinations; Semi-empirical, one-parameter model

---

*Accepted on December 04th, 2020 for publication in *Modern Physics Letters A*.
†Corresponding author. E-mail: emil@cbpf.br, emildelimamedeiros@gmail.com

1 Introduction

The existence of an isomeric state in ^{178}Hf isotope of long half-life ($T_{1/2} > 10$ yr), high spin-parity (16^+), and high excitation energy (~ 2.5 MeV) was reported for the first time as a result of a long-term experiment carried out by Helmer and Reich [1]. Subsequently, these authors measured the half-life of ^{178}Hf^{m2} (16^+) isomer as (31 ± 1) yr [2], and its excitation energy was determined more precisely as (2447.5 ± 2.5) keV by De Boer *et al.* [3] (the value accepted today is (2446.09 ± 0.08) keV [4]). Different aspects of the de-excitation mechanisms by spontaneous gamma quantum emission for the referred Hafnium isomer have been investigated until a recent past [5].

The exotic characteristics of a long half-life combined with a high excitation energy and spin makes ^{178}Hf^{m2} (16^+, 31 yr) a special and unique isomeric state in the sense that possible particle decay modes, such as α-, β^--, and ε- (electron capture) decay, and spontaneous fission as well could be considered. In the case for α-decay Van Klinken *et al.* [6] attained experimentally a lower limit of $T^{\alpha}_{1/2} > 0.6$ Gyr (α-branching ratio $< 5 \times 10^{-8}$).

It was only in 2005 that a group of researchers from the Flerov Laboratory of Nuclear Reactions (Dubna, Russia), in collaboration with Dr. J.J. Carroll of Youngstown State University (Ohio, USA), began a theoretical and experimental investigation aimed at determining the partial α-decay half-life, $T^{\alpha}_{1/2}$, of ^{178}Hf^{m2} isomer [7]. Firstly, based on the empirical Geiger-Nuttall-type systematics of alpha emitters extending from Nd to Pb isotopes, complemented by a systematic description for the spin hindrance of α-decay cases of large spin change (as for ^{211m}Po ($25/2^+$), ^{212m}Po (18^+), and ^{214}Rn^{m2} (8^+) isomers), the authors were able to estimate $T^{\alpha}_{1/2}$-values for α-transitions of ^{178}Hf^{m2} populating the energy levels of the ^{174}Yb rotational band. Results indicated a total $T^{\alpha}_{1/2}$ estimated as 0.064 Gyr, *i.e.*, about nine times lower than the lower limit previously reported [6], and the most likely modes of α-transitions as $\ell = 10$ (53%), $\ell = 8$ (23%), and $\ell = 12$ (19%) (details of the estimates are reported in [7]).

At the same time, the researchers at the Flerov Laboratory in Dubna were developing an experiment that could measure an alpha activity as low as the expected for ^{178}Hf^{m2} isomer. The Dubna group had prepared years earlier a source containing $\sim 3.5 \times 10^{13}$ atoms of ^{178}Hf^{m2} from chemical separation on a Ytterbium target enriched in ^{176}Yb isotope previously bombarded with a 36-MeV ^{4}He-ion beam according to the ^{176}Yb $(\alpha, 2n)$ reaction [8]. A first measurement was performed using a calibrated Si surface barrier detector by placing the ^{178}Hf^{m2} source and detector in good geometry inside a vacuum chamber for two weeks, resulting in a lower limit of $T^{\alpha}_{1/2} > 6.6$ Gyr [7], *i.e.*, improving by ~ 10 times the one reported by Van Klinken *et al.* [6].

Another experiment was then conducted by Karamian *et al.* [7], this time by making use of high-quality foils of CR-39 as alpha particle track detectors. Basically, the method consisted of placing the $^{178}\mathrm{Hf}^{m2}$ source between two plates of CR-39 and sealed the sandwich for a convenient period of exposure time. By taking care against excessive damage after etching (choosing appropriate exposure time and adjusting the etching procedure to make visible the alpha particle tracks clearly) and the background tracks registered on the detector surface not exposed to the active source, such a detection method allowed, after an exposure of about one year, to reach a value of $T^{\alpha}_{1/2} = (25 \pm 5)$ Gyr for the α-decay of $^{178}\mathrm{Hf}^{m2}$ isomer, which value is compatible with the result previously obtained with Si detector, but 390 times larger than the estimated value [7].

In view of the significant differences shown in the $T^{\alpha}_{1/2}$-values mentioned above, and since the literature does not provide other indications of $T^{\alpha}_{1/2}$ for $^{178}\mathrm{Hf}^{m2}$ isomer, either theoretically or experimentally, we decided therefore to apply our semi-empirical calculation model of heavy-particle decay [9–12] to obtain an alternative estimate of such a quantity. The present study complements our recent paper reporting on a reinvestigation of alpha-decay half-lives of all α-emitting Hf isotopes [13].

2 The model

The methodology used in the present work to calculate half-lives for heavy-particle radioactivity (nuclear decay by one- and two-proton emission, α-decay, and cluster emission processes) is based on the quantum mechanical tunneling mechanism through a potential barrier as first proposed by Gamow [14] and Gurney and Condon [15, 16]. Here, the Coulomb, centrifugal, and overlapping barriers have been considered separately in the spherical nucleus approximation. The description of the model was done for the first time in 2005 to obtain an estimate for the α-decay half-life of ^{209}Bi isotope [9], which showed good agreement with the measured half-life value determined by de Marcillac *et al.* [17]. A number of applications of the model to different cases of heavy-particle radioactivity are quoted in our recent paper devoted to a reinvestigation of α-decay of Hafnium isotopes [13], where details of this semi-empirical, one-parameter model have been also reported.

In what follows subscripts P and D refer to parent emitter and daughter product nuclei, respectively. According to our calculation model, for a given α-particle decay case, the half-life, $\tau = \log_{10} T_{1/2}$, is obtained from the summation

$$\tau = \log_{10} T^{\alpha}_{1/2} = \tau_{\mathsf{fa}}(Q_\alpha) + \tau_{\mathsf{ov}}(Q_\alpha, \ell, g) + \tau_{\mathsf{coul}}(Q_\alpha) + \tau_{\mathsf{cent}}(Q_\alpha, \ell)\,, \tag{1}$$

where τ_{fa} is the contribution due to the frequency of assaults to the barrier, and τ_{ov} comes from the semi-classical WKB-integral approximation calculated in the overlapping barrier region where the α-particle drives away from the parent nucleus until the configuration of contact at the nuclear surface. The sum $\tau_{\mathsf{coul}} + \tau_{\mathsf{cent}} = \tau_{\mathsf{se}}$ comes from the semi-classical WKB-integral approximation calculated through the external, separation barrier region formed by the Coulomb-plus-centrifugal contributions. Q_α denotes the total energy available in the α-decay process, and ℓ represents the minimum value of the mutual orbital angular momentum of the product nuclei around their common center of mass.

The main expressions to be used in calculating the various quantities in Eq. (1) are here reproduced from our previous paper [13] (note that lengths and distances are expressed in fm, masses in u (atomic mass unit), energies in MeV, and time in year (yr)):

$$\tau_{\mathsf{fa}} = -29.5 + \log_{10}\left[a \cdot (\mu_0/Q_\alpha)^{1/2}\right] , \tag{2}$$

$$\tau_{\mathsf{ov}} = g \cdot \tau_1, \quad \tau_1 = 0.19 \cdot (c-a) \cdot (\mu_0 \cdot Q_\alpha)^{1/2} \cdot H(x,y) , \tag{3}$$

$$\tau_{\mathsf{coul}} = 0.54716 \cdot Z_{\mathrm{D}} \cdot (\mu_0/Q_\alpha)^{1/2} \cdot F(0,y) , \quad \text{and} \tag{4}$$

$$\tau_{\mathsf{cent}} = \tau_{\mathsf{coul}} \cdot [F(x,y)/F(0,y) - 1] . \tag{5}$$

Here, $a = R_{\mathrm{P}} - R_\alpha$, where $2a$ represents the linear displacement of the α-particle between two successive assaults to the barrier, and $c = R_{\mathrm{D}} + R_\alpha$ defines the configuration at contact of the preformed fragments (daughter nucleus and emitting α-particle). In this way, the length $c - a = 2R_\alpha - (R_{\mathrm{P}} - R_{\mathrm{D}})$ gives the width of the overlapping barrier region (see Fig. 1-a).

The routine calculation to estimate nuclear radius, R_i (i = P, D), has followed the finite range droplet model of atomic nuclei as it has been described by Möller *et al.* [18], where the spherical approximation of the nuclear volume has been adopted in the present analysis (see also [19]). This nuclear radius parametrization has been updated recently by Möller *et al.* [20]. The new radius data have been obtained from a significantly improved treatment that took into account more accurate experimental ground-state nuclear mass data [20]. The expressions that enable to calculate the average equivalent root-mean-square radius of the proton, Q_{p}, and neutron, Q_{n}, density distributions,

$$R_i \equiv \overline{Q_{\mathrm{Z,A}}} = (Z/A)\, Q_{\mathsf{p}} + (1 - Z/A)\, Q_{\mathsf{n}} , \;\; i = \mathrm{P, D} , \tag{6}$$

have been reported elsewhere [12, 13]. This procedure reveals that the ratio $r = R/A^{1/3}$ decreases a little when one passes from intermediate-mass to heavy nuclei, thus indicating a clear degree of nuclear compressibility, making, therefore, the simple radius formula $R = r \cdot A^{1/3}$ not valid in estimating nuclear radius in the whole range of mass number.

Concerning the alpha-particle radius, it has been adopted the value $R_\alpha = (1.62 \pm 0.01)$ fm, in accordance to the α-particle radius-value derived from the charge density distribution measured by

Sick *et al.* [21] in electron scattering experiments on ^{4}He target. Excellent reproducibility of alpha-decay data was attained using the above mentioned R_α-value coupled with a simple Gamow's-like model applied to a large number (more than three hundred cases) of measured alpha-decay half-lives covering the mass-number interval $106 \leq A \leq 264$ [22].

The only adjustable parameter of the model, g, results from a combination of exponents p and q,

$$g = [1 + (p+q)/2]^{-1}\,, \;\; 0 < g \leq 2/3\,, \tag{7}$$

of two assumed power functions to describe the reduced mass of the disintegrating system, $\mu(s)$, and the potential barrier, $V(s)$, respectively, in the overlapping barrier region, $a \leq s \leq c$ (s is the distance of separation between the centers of the forming product nuclides). The g-value depends upon the source of input data for both nuclear mass and radius, the adopted values for the different physical constants, and, of course, the measured half-life data of a given set of alpha-decay cases. Once a mass table and/or a nuclear radius parametrization were chosen, subsequent half-life determinations should be done using these sources of data for mass- and radius-values as well as the physical constants with which the g-value was obtained. Parameter g is related to the strength of the spectroscopic factor, *i.e.*, the α-particle preformation probability, whose value is given by $S = 10^{-g\cdot\tau_1}$ (see Eq. (3)).

The Q_α-value and effective reduced mass, μ_0, of the disintegrating system have been obtained by

$$Q_\alpha = m_{\rm P} - (m_{\rm D} + m_\alpha)\,, \quad \text{and} \quad \mu_0 = \left(m_{\rm D}^{-1} + m_\alpha^{-1}\right)^{-1}\,, \tag{8}$$

where the m's represent nuclear (rather than atomic) masses, calculated by the usual way, namely

$$m_i = A_i - Z_i \cdot m_{\rm e} + \left(\Delta M_i + kZ_i^\beta\right)/F, \quad i = \text{P, D}. \tag{9}$$

Here, $m_{\rm e} = 0.54857990907 \times 10^{-3}$ u is the electron rest mass, $m_\alpha = 4.001506179127$ u is the alpha particle mass, $\Delta M_i'$s are the atomic mass-excess values (expressed in MeV) as tabulated in [23], kZ_i^β represents the total binding energy of the Z electrons in the atom, and $F = 931.4940038$ MeV/u is the mass-energy conversion factor. The k- and β-values come from an analysis of calculated data for electron binding energies of neutral atoms by Huang *et al.* [24]. From the analysis it is obtained

$$k = 8.7 \times 10^{-6}\,\text{MeV and } \beta = 2.517, \quad \text{for nuclei of} \quad Z \geq 60. \tag{10}$$

$$k = 13.6 \times 10^{-6}\,\text{MeV and } \beta = 2.408, \quad \text{for nuclei of} \quad Z < 60. \tag{11}$$

For the general case of α-transitions from an α-emitter nuclide in an excited state at $E^*_{\rm P}$ to a product, daughter nuclide in an excited state at $E^*_{\rm D}$, Q_α-value has been calculated by

$$Q_\alpha = \Delta M_{\rm P} - \Delta M_{\rm D} - 2.42491561 + W + E^*_{\rm P} - E^*_{\rm D} \;\text{MeV}\,, \tag{12}$$

where the $\Delta M'$s refer to ground-state nuclides, and

$$W = \left[8.7 \cdot \left(Z_{\rm P}^{2.517} - Z_{\rm D}^{2.517}\right) - 72.18\right] \cdot 10^{-6}\,\text{MeV},\ Z_i \geq 60\ \ (i = \text{P, D}) \tag{13}$$

is the screening effect to the nuclei caused by the surrounding electrons.

Finally, the functions $H(x, y)$ and $F(x, y)$ contain the dependence upon mutual angular momentum, ℓ (if any), which comes from the nuclear spin ($\boldsymbol{J}$) and parity (π) conservation laws ($\boldsymbol{J}_{\rm P} = \boldsymbol{J}_{\rm D} + \boldsymbol{J}_\alpha + \boldsymbol{\ell}$, $\pi_{\sf P} = \pi_{\sf D} \cdot \pi_\alpha \cdot (-1)^\ell$) to the α-decay process. These functions are written as

$$H(x, y) = (x + 2y - 1)^{1/2}, \tag{14}$$

$$F(x, y) = \frac{x^{1/2}}{2y} \cdot \ln \frac{x^{1/2} H(x, y) + x + y}{\sqrt{x + y^2}} + \arccos \left\{ \frac{1}{2} \cdot \left[1 - \frac{y - 1}{\sqrt{x + y^2}} \right] \right\}^{1/2} - \frac{H(x, y)}{2y}\,, \tag{15}$$

and the quantities x and y are defined as

$$x = 20.9008 \cdot \ell(\ell + 1)/(\mu_0 \cdot c^2 \cdot Q_\alpha), \quad y = Z_{\rm D} e^2/(c \cdot Q_\alpha)\,. \tag{16}$$

Here, $e^2 = 1.43996444$ MeV·fm is the square of the electronic elementary charge, and expressions (14) and (15) are valid for all values of $x \geq 0$, $y > 1/2$.

In cases for which $\ell = 0$ it results $x = 0$, $\tau_{\sf cent} = 0$, and, in addition,

$$\tau_1 = 0.19 \cdot (c - a) \cdot \left[\mu_0 \cdot Q_\alpha \cdot (u^{-1} - 1)\right]^{1/2}, \text{ and} \tag{17}$$

$$F(0, y) = \arccos u^{1/2} - [u \cdot (1 - u)]^{1/2}\,,\ u^{-1} = 2y\,. \tag{18}$$

3 Preliminary predictions

Different levels of excitation and spin-parity of ^{174}Yb can be populated by α-transitions from ^{178}Hf^{m2} parent isomer ($J^\pi = 16^+, E_{\rm P}^* = 2.44609$ MeV). The energy levels of the ground-state band of ^{174}Yb increase from (0 keV, 0^+) up to (2457 keV, 14^+) [25], so that such α-transitions exhibit high Q_α-values which decrease from ~ 4.56 MeV down to ~ 2.10 MeV, at the same time that the corresponding spin changes (angular momentum) also decrease from $\ell = 16$ down to $\ell = 2$.

It is not difficult to identify the energy level (or levels) that should be the most populated ones as a result of the α-transitions mentioned above. In fact, according to the current tunneling mechanism through a potential barrier to α-decay, the half-life can be expressed as

$$\tau = \log_{10} T_{1/2}^\alpha = \log\left[(\ln 2)/\lambda_0\right] + (G_{\sf ov} + G_{\sf se}) \cdot 0.4343\,, \tag{19}$$

where $\lambda_0 \approx (1.6\text{–}2.3) \times 10^{21}\,\mathrm{s}^{-1}$ represents the frequency of assaults on the barrier, and G_{ov} and G_{se} are the semi-classical WKB-integral approximations (Gamow factors) calculated in the overlapping and separation regions, respectively (see Fig. 1-b).

The first term in (19) is practically constant (a variation of only ~ 0.16) because λ_0 does not vary significantly. Therefore, the trend of τ is essentially dictated by the quantity $G_{\mathsf{ov}} + G_{\mathsf{se}}$, which is given by

$$G_{\mathsf{ov}} + G_{\mathsf{se}} = \left[(8\mu_0)^{1/2}/\hbar\right] \times G_{\mathsf{r}}\,, \quad G_{\mathsf{r}} = \int_a^c f_{\mathsf{ov}}(s)\,\mathrm{d}s + \int_c^b f_{\mathsf{se}}(s)\,\mathrm{d}s \tag{20}$$

$$\text{with} \qquad f_{\mathsf{ov}}(s) = Q_\alpha^{1/2} \cdot H(x,y) \cdot (c-a)^{-\nu} \cdot (s-a)^{\nu} \tag{21}$$

$$\text{and} \qquad f_{\mathsf{se}}(s) = Q_\alpha^{1/2} \cdot \left[xc^2/s^2 + 2yc/s - 1\right]^{1/2}, \tag{22}$$

as in the example shown in Fig. 1-b. In these expressions, b is the outer turning point obtained from the condition $f_{\mathsf{se}}(b) = 0$, which gives

$$b = c \cdot \left[y + (x + y^2)^{1/2}\right], \tag{23}$$

and $\nu > 1/2$ is an unknown parameter. We will call $G_{\mathsf{r}} = G_{\mathsf{r}}^{\mathsf{ov}} + G_{\mathsf{r}}^{\mathsf{se}}$ (definition (20)) as reduced Gamow factor.

The first integral in (20) is the area of the overlapping region (shaded region in Fig. 1-b),

$$G_{\mathsf{r}}^{\mathsf{ov}} = Q_\alpha^{1/2} \cdot H(x,y) \cdot (c-a) \cdot (\nu+1)^{-1}\,. \tag{24}$$

Since ν is still unknown and, in addition, calculations have indicated that $G_{\mathsf{r}}^{\mathsf{ov}}/G_{\mathsf{r}} \leq 10\%$, $G_{\mathsf{r}}^{\mathsf{ov}}$ has been approximated to the area of the triangle of base $c - a$ and height $f_{\mathsf{se}}(c)$, *i.e.*,

$$G_{\mathsf{r}}^{\mathsf{ov}} \approx \frac{1}{2}(c-a) \cdot Q_\alpha^{1/2} \cdot H(x,y)\,. \tag{25}$$

On the other hand, the area of the separation region ($c \leq s \leq b$ in Fig. 1-b) can be calculated exactly to give

$$G_{\mathsf{r}}^{\mathsf{se}} = c\,Q_\alpha^{1/2} \cdot \left[x^{1/2} \cdot \ln \frac{x^{1/2} H(x,y) + x + y}{\sqrt{x+y^2}} + y \cdot \arccos \frac{1-y}{\sqrt{x+y^2}} - H(x,y)\right] \tag{26}$$

(recall that $H(x,y)$ is defined by (14), and x and y by (16)).

Results of $G_{\mathsf{r}} = G_{\mathsf{r}}^{\mathsf{ov}} + G_{\mathsf{r}}^{\mathsf{se}}$ calculated in this way are reported in Table 1 for the modes of α-decay of $^{178}\mathrm{Hf}^{m2}$ isomer to levels of the ground-state band of $^{174}\mathrm{Yb}$. Since $T_{1/2}^{\alpha}$ increases quite exponentially with G_{r}, this latter quantity can serve to anticipate the most probable modes of α-decay to occur.

The lower G_{r} the more likely is its corresponding α-transition. For the case under analysis Table 1 indicates the α-transitions of $\ell = 10$, $\ell = 12$, and $\ell = 8$ (in this order) as the most likely to occur. This conclusion is partially in agreement with that found by Karamian *et al.* who reported $\ell = 10$, $\ell = 8$, and $\ell = 12$ as the order for the most probable α-transitions [7].

4 Semi-empirical parameter *g*

To determine the partial α-decay half-lives for the transitions $^{178}\mathrm{Hf}^{m2} \to {}^{174}\mathrm{Yb}^*$ the task of finding semi-empirical values for parameter g of the present calculation model must be first carried out. The set of known cases of α-decay to be used as input data should contain a number of isomeric states as parent and daughter nuclear species, decays with spin differences as high as $\ell = 16$ or greater, and should cover a large interval of half-life values. Table 2 lists the main data for twenty-nine cases of selected α-decays of $63 \leq Z \leq 98$, $151 \leq A \leq 251$, $0 \leq \ell \leq 18$, covering e-e, e-o, o-e, and o-o nuclei, 38 % of the cases being isomeric α-decays, and a variation of thirty-seven orders of magnitude in half-life.

Then, by using (1)–(5), one derives

$$g^{\mathsf{e}} = \left(\tau^{\mathsf{e}} - \tau_{\mathsf{fa}} - \tau_{\mathsf{coul}} - \tau_{\mathsf{cent}}\right)/\tau_1 \, , \tag{27}$$

from which the g^{e}-values have been deduced (superscript "e" indicates that the g-values come from experimental data, and τ^{e} from experiments). Table 2 reports in the last column the semi-empirical g^{e}-values thus obtained. It is seen that all g^{e}-values resulted within the range $0 < g \leq 2/3$ allowed by the present model.

As expected, there should be a dependence of g^{e} upon ℓ. To find this dependence, firstly the fourteen g^{e}-values of $\ell = 0$ have been replaced by their average value, $\overline{g_0^{\mathsf{e}}} = 0.161 \pm 0.021$. In addition, the same was done for the six cases of $\ell = 2$, four cases of $\ell = 5$, and two cases of $\ell = 6$, thus obtaining $\overline{g_2^{\mathsf{e}}} = 0.217 \pm 0.029$, $\overline{g_5^{\mathsf{e}}} = 0.474 \pm 0.062$, and $\overline{g_6^{\mathsf{e}}} = 0.532 \pm 0.035$, respectively.

In this way, the initial set of twenty-nine pairs of g^{e}- and their associated ℓ-values has been reduced to seven ones. These points are plotted in Fig. 2, through which points a smooth curve by eye fit has been drawn. In this way, estimated g^{c}-values for $0 \leq \ell$-values < 20 have been picked out from the curve of Fig. 2 within $\sim 10\,\%$ of average uncertainty.

5 Calculated partial alpha-decay half-life

The calculated α-decay, $T^{\mathsf{c}}_{1/2}$ (or $\tau^{\mathsf{c}} = \log_{10} T^{\mathsf{c}}_{1/2}$) can now be obtained for *i*) all cases listed in Table 2, and *ii*) the eight α-transitions $^{178}\mathrm{Hf}^{m2} \to {}^{174}\mathrm{Yb}^{*}$ of $\ell = 2, 4, \ldots 16$. It suffices to insert back into (3) the calculated (or estimated) g^{c}-values as described above and then make the summation (1).

Defining the calculated "reduced" half-life, $\tau^{\mathsf{c}}_{\mathsf{r}}$, and experimental "reduced" half-life, $\tau^{\mathsf{e}}_{\mathsf{r}}$, by subtracting from the half-life τ (Eq. (1)) all its contributions other than the Coulomb one, *i.e.*,

$$\tau^{\mathsf{c}}_{\mathsf{r}} = \tau^{\mathsf{c}} - (\tau_{\mathsf{fa}} + g^{\mathsf{c}} \cdot \tau_1 + \tau_{\mathsf{cent}}) \quad \text{and} \quad \tau^{\mathsf{e}}_{\mathsf{r}} = \tau^{\mathsf{e}} - (\tau_{\mathsf{fa}} + g^{\mathsf{c}} \cdot \tau_1 + \tau_{\mathsf{cent}})\,, \tag{28}$$

one has

$$\Delta\tau_{\mathsf{r}} = \tau^{\mathsf{c}}_{\mathsf{r}} - \tau^{\mathsf{e}}_{\mathsf{r}} = \tau^{\mathsf{c}} - \tau^{\mathsf{e}} = \Delta\tau\,. \tag{29}$$

Definition (28) means that $\tau^{\mathsf{c}}_{\mathsf{r}} = \tau_{\mathsf{coul}} = C \cdot z$, where $C = 0.54716$, $z = Z_{\mathrm{D}} \cdot (\mu_0/Q_\alpha)^{1/2} \cdot F(0, y)$ and, therefore, it does not depend upon ℓ. On the other hand, from (1) and (3) one has $\Delta\tau = \tau_1 \cdot \Delta g$, which combined with (29) gives

$$\tau^{\mathsf{e}}_{\mathsf{r}} = C \cdot z - \tau_1 \cdot (g^{\mathsf{c}} - g^{\mathsf{e}}). \tag{30}$$

In this way, both sets *i*) and *ii*) of decay cases mentioned above can be displayed in a linear form when the quantities $\tau^{\mathsf{c}}_{\mathsf{r}}$ and $\tau^{\mathsf{e}}_{\mathsf{r}}$ are plotted against $z = Z_{\mathrm{D}} \cdot (\mu_0/Q_\alpha)^{1/2} \cdot F(0, y)$, where $F(0, y)$ is given by (18).

Figure 3 displays the reduced α-decay half-life data following the present methodology for the twenty-nine decay cases selected (Table 2) that have been used to obtain the variation of the semi-empirical parameter g^{c} with ℓ. It is found that in 93 % of cases $0.010 < |\tau^{\mathsf{c}} - \tau^{\mathsf{e}}| < 0.270$, *i.e.*, a ratio of $T^{\mathsf{c}}_{1/2}$ to $T^{\mathsf{e}}_{1/2}$ less than ~ 1.9, with the observation that in twenty cases the calculated and experimental half-life values differ from each other by less than 50 %. The smallest differences (less than ~ 7 %) are found for $^{152}\mathrm{Ho}^{m}$, $^{157}\mathrm{Lu}^{m}$, $^{186}\mathrm{Os}$, and $^{218}\mathrm{U}^{m}$ parent nuclei, and for $^{237}\mathrm{Np}\,(5/2^+) \to {}^{233}\mathrm{Pa}\,(5/2^+)$, $^{239}\mathrm{Pu}\,(1/2^+) \to {}^{235}\mathrm{U}\,(1/2^+)$, and $^{239}\mathrm{Pu}\,(1/2^+) \to {}^{235}\mathrm{U}\,(3/2^+)$ α-decays. Only in two cases (filled squares near $z \approx 53$ in Fig. 3 for $^{251}\mathrm{Cf}$ parent nucleus) did the ratio of $T^{\mathsf{c}}_{1/2}$ to $T^{\mathsf{e}}_{1/2}$ become ~ 3. However, it should be noted that the data analyzed here cover a range of thirty-seven orders of magnitude in half-life.

Agreement between calculated and experimental half-life-values for the twenty-seven cases mentioned above can be considered quite satisfactory, mainly because six of them (located in $15 < z < 35$) are α-transitions of $5 \leq \ell \leq 18$, which makes the present estimates of g^{c} reliable for the purposes of this study. In the case for $^{212}\mathrm{Po}^{m} \to {}^{208}\mathrm{Pb}^{g}$ ($\ell = 18$) α-decay (semi-darkened point at $z = 16.2$), for instance, one obtained $T^{\mathsf{c}}_{1/2}/T^{\mathsf{e}}_{1/2} \approx 1.27$. Results of partial α-decay half-life of cases of special interest of the present work are reported in Table 3, where the last two columns show $T^{\mathsf{c}}_{1/2}$ and α-intensity with which the levels of ^{174}Yb daughter are expected to be populated. And in Fig. 3 the half-life data are also presented in the form of reduced half-life by open circles which represent calculated $\tau^{\mathsf{c}}_{\mathsf{r}}$-values, and that are located on the $\tau^{\mathsf{c}}_{\mathsf{r}} = C \cdot z$ line.

The total alpha half-life combining all cases listed in Table 3 has resulted as $T^{\alpha}_{1/2} = (0.24 \pm 0.07)$ Gyr. According to the present analysis, the most frequent α-transitions from ^{178}Hf^{m2} are to levels of ^{174}Yb when $\ell = 10\,(16^+ \to 6^+, Q_\alpha \approx 4.032\,\mathrm{MeV}, 57\,\%)$, $\ell = 12\,(16^+ \to 4^+, Q_\alpha = 4.305\,\mathrm{MeV}, 36\,\%)$, and $\ell = 8\,(16^+ \to 8^+, Q_\alpha = 3.669\,\mathrm{MeV}, 4.7\,\%)$, thus confirming the previous prediction reported in Table 1. These results differ slightly from those of Karamian *et al.* [7], who have indicated $\ell = 10\,(\sim 53\,\%)$, $\ell = 8\,(\sim 23\,\%)$, and $\ell = 12\,(\sim 19\,\%)$ as the most likely modes of α-decay [7]. Also, the total $T^{\alpha}_{1/2}$ estimated by the present methodology resulted higher than the one reported in [7] by a factor just under 4, and $\sim (100 \pm 35)$ times lower than the value obtained experimentally in [7]. The fact that the two estimates of $T^{\alpha}_{1/2}$ for ^{178}Hf^{m2} isomer are relatively close to each other may be an indication of some fault in the experiment described in [7], since a high measured $T^{\alpha}_{1/2}$-value may be indicative of loss of events in the detector, which may be related to uncertainties in the determination of the detection efficiency, or eventually to other causes.

Additionally, $T^{\alpha}_{1/2}$-data of Table 3 are also shown in graphical form (Fig. 4) to make easier to understand how does $T^{\alpha}_{1/2}$ varies upon the physical caracteristics (Q_α, ℓ) which govern each of the eight α-transitions. In Fig. 4 it can be seen that the quantity τ_{fa} is almost constant (a decrease of only $\sim 0.6\,\%$). Both τ_{ov} and τ_{cent} increase significantly. The former increases by a factor ~ 3.6 due to simultaneous increasing of parameter g and ℓ, while the latter (an increasing by a factor ~ 39) to a rapid increasing of the term $\ell \cdot (\ell + 1)$. Recall that the probability of preforming of the disintegration products is given by $S = 10^{-\tau_{\mathsf{ov}}}$, therefore S shows a decreasing from ~ 0.06 down to $\sim 3.7 \times 10^{-5}$. Finally, the decreasing seen in τ_{coul}-values exceeds the increasing of τ_{ov} plus τ_{cent} until it reaches the minimum in $Q_\alpha \approx 4.032$ MeV and $\ell = 10$, when then the half-life $\tau^{\mathsf{c}} = \tau_{\mathsf{fa}} + \tau_{\mathsf{ov}} + \tau_{\mathsf{coul}} + \tau_{\mathsf{cent}}$ starts to increase, showing that the effect of Q_α on τ^{c} is stronger than the hindrance created by ℓ until $\ell = 10$. This is the first time the four components τ_{fa}, τ_{ov}, τ_{cent}, and τ_{coul} are depicted to some detail.

6 Towards a systematization of α-decay half-life

The observation that both the quantity associated to the frequency of assaults on the potential barrier, $\tau_{\mathsf{fa}} = \log\left[(\ln 2)/\lambda_0\right]$, and $\mu_0^{1/2}$ can be considered constant within $\sim 0.6\,\%$ for the α-emitting isotopes along the Nuclide Chart, led us to search for a single correlation between half-life $\tau =$

$\log_{10} T^{\alpha}_{1/2}$ and reduced Gamow factor $G_{\mathsf{r}} = G^{\mathsf{ov}}_{\mathsf{r}} + G^{\mathsf{se}}_{\mathsf{r}}$.

Starting from eq. (19), and by comparing

$$(\log e) \cdot \left[(8\mu_0)^{1/2}/\hbar\right] \cdot G^{\mathsf{ov}}_{\mathsf{r}} = 0.19 \cdot (c-a) \cdot (\mu_0 Q_\alpha)^{1/2} \cdot H(x,y) \cdot (\nu+1)^{-1} \tag{31}$$

with (3) it results in $g = (\nu+1)^{-1}$, so that the approximate values for $G^{\mathsf{ov}}_{\mathsf{r}}$ as given by (25) is now substituted by the correct one,

$$G^{\mathsf{ov}}_{\mathsf{r}} = (c-a) \cdot g \cdot Q^{1/2}_{\alpha} \cdot H(x,y). \tag{32}$$

Therefore, the correct value for reduced Gamow factor, G_{r}, can be obtained semi-empirically, and the dependence of half-life τ upon G_{r} should appear very close to a straight line. The general expression for G_{r} (any ℓ-value) is obtained by combining (26) with (32) to give

$$G_{\mathsf{r}} = Q^{1/2}_{\alpha} \left\{ c\,x^{1/2} \cdot \ln \frac{x^{1/2} H(x,y) + x + y}{\sqrt{x+y^2}} + c\,y \cdot \arccos \frac{1-y}{\sqrt{x+y^2}} - [c-(c-a)g] \cdot H(x,y) \right\}. \tag{33}$$

In particular, for favored α-transitions of $\ell = 0$, one has

$$G_{\mathsf{r}} = Q^{1/2}_{\alpha} \left\{ c\,y \cdot \arccos\left(\frac{1}{y} - 1\right) - [c-(c-a)g]\sqrt{2y-1} \right\}. \tag{34}$$

Figure 5 shows such an expected linear relationship between τ and G_{r} achieved from a sample of twenty experimental data of $0 \leq \ell \leq 18$, α-transitions either from ground or isomeric states, irrespective of being e-e, e-o, o-e, and o-o nuclides, and covering thirty orders of magnitude in half-life (darkened points in Fig. 5; location for some α-emitting nuclides are indicated by arrows). Also plotted in Fig. 5 are the eight cases of calculated half-lives for $^{178}\mathrm{Hf}^{m2}$ isomer decaying into excited states of Yb isotopes as reported in Table 3 (open circles). From inspection of Fig. 5 it appears that the half-life is strictly related to reduced Gamow factor, G_{r}, and it works as a universal-like law which can be used to estimate half-lives of alpha transitions in general.

A few examples of using of the dependence τ *vs* G_{r} in Fig. 5 to obtain calculated α-decay half-life values are given in Table 4, where it is seen that calculated values differ from the measured ones by no more than a factor ~ 2 (two exceptions are for $^{152}\mathrm{Gd}$ and $^{202}\mathrm{At}^{m}$ α-emitters). The single formula

$$\tau^{\mathsf{c}} = \log T^{\mathsf{c}}_{1/2} = (0.3805 \pm 0.0014) \cdot G_{\mathsf{r}} - (29.23 \pm 0.12) \tag{35}$$

can then be used to estimate half-lives for α-transitions with uncertainties not greater than a factor ~ 4, whatever the value of ℓ, the type (e-e, e-o, o-e, or o-o) of α-emitting nuclide, and whether the transition occurs from the ground or isomeric states of the parent nucleus. A better accuracy in α-decay half-life estimates by a formula like (35) can be achieved from a much larger sample of measured data than the input data of Table 2 that have been used in the present analysis.

It is worth mentioning that very recently Deng, Zhang, and Royer [32] have published their results on an improved general α-decay half-life systematics covering 606 alpha-emitter nuclides (ground and isomer states) where the blocking effect of unpaired nucleons has been also incorporated into the analysis. With only eight adjustable parameters such a study showed that $\sim 96\,\%$ of all measured data have been reproduced with standard deviation of $\sigma = 0.356$.

7 Final comments and conclusion

In this paper a semi-empirical calculation model based on the quantum mechanical tunneling mechanism through a potential barrier is applied to rare cases of α-transitions from a parent, α-emitter nuclear species at an isomeric state of very high spin ($J = 16^+$) and excitation energy ($E^* = 2446\,\text{keV}$): this is the case for $^{178}\text{Hf}^{m2}$ ($T_{1/2} = 31\,\text{yr}$) isomer decaying to the energy levels of the ground-state rotational band of ^{174}Yb daughter isotope.

There are other studies directly related to α-decay from nuclear isomeric states. For instance, the effective liquid drop model-ELDM of heavy-particle radioactivity [33] has been successfully applied, by Zhang and Ren [34], in obtaining α-decay half-lives of ground and isomeric states in a unified theoretical framework to a variety of heavy and super-heavy parent nuclei. In a more recent past, a generalization of Geiger-Nuttal law for α-decay of heavy nuclei has been developed by Ren and Ren (the so-called new Geiger-Nuttal law) [35], with which the α-decay half-lives of the high-spin isomers of ^{212}Po have been well reproduced.

The present study has revealed that the most likely alpha transitions to occur from $^{178}\text{Hf}^{m2}$ isomer are those of angular momentum $\ell = 10\,(\sim 57\,\%)$, $\ell = 12\,(\sim 36\,\%)$, and $\ell = 8\,(\sim 4.4\,\%)$ corresponding to half-lives of (0.43 ± 0.18) Gyr, (0.68 ± 0.30) Gyr, and (5.2 ± 2.1) Gyr, respectively, and a partial half-life for all modes of α-decay as $T^{\alpha}_{1/2} = (0.24 \pm 0.07)$ Gyr. Considering the rarity of the α-decay case under investigation, and the uncertainties associated with the various quantities involved in the calculations, the above results differ little from those previously found by Karamian *et al.* [7] who report $\ell = 10\,(\sim 53\,\%)$, $\ell = 8\,(\sim 23\,\%)$, and $\ell = 12\,(\sim 19\,\%)$ for the most likely α-transitions, and a total α-decay half-life estimated as $T^{\alpha}_{1/2} = 0.064$ Gyr, thus differing from the present calculated result by a factor $\sim 3.7 \pm 1.1$.

However, both $T^{\alpha}_{1/2}$-values quoted above do not agree with the unique measured value for

$^{178}\mathrm{Hf}^{m2}\,(16^+) \to \mathrm{Yb}^*\,(0^+,\,2^+,\,\ldots\,,14^+)$ decays available in the literature, $(25 \pm 5)\,$Gyr, which was also achieved by Karamian *et al.* [7], differing from their estimated value by a factor ~ 390, but only by two orders of magnitude from the present estimate. Clearly, new experiments on this subject using alternative α-particle detection methods, as well as other theoretical and/or semi-empirical approaches that can lead eventually to more reliable estimates, are needed for clarifying the differences in half-life values mentioned above for such an exotic α-disintegration process.

In the present semi-empirical calculation model, besides the usual Coulomb and centrifugal contributions to the potential barrier, it is taken into account the overlapping region of the nascent fragments where both the reduced mass and the potential barrier for the disintegrating system have been described by power functions of unknown exponents, p and q, respectively, thus leading to an adjustable parameter of the model, $g = [1 + (p+q)/2]^{-1}\,(0 < g \leq 2/3)$. It should be noted that the value of this single, semi-empirical parameter found by this methodology depends on the sample of α-decay cases to be analyzed, as well as the choice for the data source of mass-excess values of the nuclei involved, and the parameterization to be used in determining the nuclear radii as well.

Firstly, the WKB integrals were used in tunneling through the potential barriers of both the overlapping and separation regions (including the centrifugal contribution) to obtain the reduced Gamow factor, $G_{\mathsf{r}} = G_{\mathsf{r}}^{\mathsf{ov}} + G_{\mathsf{r}}^{\mathsf{se}}$, as an indicator for the α-transitions most likely to occur from $^{178}\mathrm{Hf}^{m2}$ isomer. Then, from a sample of twenty-nine alpha-decay cases of e-e, e-o, o-e, and o-o nuclei covering a large range of Z, A, ℓ, and a variation of thirty-seven orders of magnitude in the measured half-life values, including cases of alpha-emitting isomers, a correlation between parameter g and angular momentum ℓ was constructed (Fig. 2), thus making it possible to estimate the half-lives of the α-transitions from $^{178}\mathrm{Hf}^{m2}$ parent isomer into the different energy levels of the ground state rotational band of Yb daughter isotope. Results confirmed the preliminary prediction about the most favorable α-decay modes, also allowing through the use of this methodology to obtain the total α-disintegration half-life of $^{178}\mathrm{Hf}^{m2}$ isomer as two orders of magnitude lower than the value measured in [7]. Besides, for the first time a detailing of the different parts that compose the calculated half-life for each decay mode has been reported (Fig. 4).

Additionally, as a byproduct of this analysis, it was possible to establish the expected linear correlation between α-decay half-life, $\tau = \log T^{\alpha}_{1/2}$, and reduced Gamow factor, G_{r} (Fig. 5), which, like g *vs* ℓ correlation (Fig. 2), is not absolute, although both may have a universal character.

Finally, we believe that the present calculation model will be useful in predicting half-lives of other possible α-active isomeric states (if any), as well as in the α-disintegration chains of super-heavy nuclei, both those synthesized and the ones not yet artificially produced. We want to conclude with two examples for this latter research area by noting in Table 4 that the observed α-decay half-lives for both ^{293}Ts and ^{294}Og super-heavy nuclei have been satisfactorily well reproduced by the present semi-empirical approach.

References

[1] R. G. Helmer and C. W. Reich, Decay of an isomeric state in ^{178}Hf with $K \geq 16$, *Nucl. Phys. A* **114**, 649 (1968).

[2] R. G. Helmer and C. W. Reich, Half-life of $^{178}\mathrm{Hf}^{m2}$ and its neutron capture production, *Nucl. Phys. A* **211**, 1 (1973).

[3] F. W. N. De Boer, P. F. A. Goudsmit, B. J. Meijer, J. C. Kapteyn and J. Konijn, The four quasi-particle ^{178}Hf isomeric state, its excitation energy and multipolarities of deexciting transitions, *Nucl. Phys. A* **263**, 397 (1976).

[4] G. Audi, F. G. Kondev, M. Wang, W. J. Huang and S. Naimi, The NUBASE2016 evaluation of nuclear properties, *Chin. Phys. C* **41**, 030001 (2017).

[5] M. B. Smith *et al.*, γ rays emitted in the decay of 31-yr $^{178}\mathrm{Hf}^{m2}$, *Phys. Rev. C* **68**, 031302 (2003).

[6] J. Van Klinken, W. Z. Venema, R. V. F. Janssens and G. T. Emery, K-forbidden decays in ^{178}Hf; M4 decay of an Yrast state, *Nucl. Phys. A* **339**, 189 (1980).

[7] S. A. Karamian, J. J. Carroll, S. Iliev and S. P. Tretyakova, Weak K hindrance manifested in α decay of the $^{178}\mathrm{Hf}^{m2}$ isomer, *Phys. Rev. C* **75**, 057301 (2007).

[8] Yu. Ts. Oganessian *et al.*, Production, chemical and isotope separations of the long-lived isomer $^{178}\mathrm{Hf}^{m2}$ ($T_{1/2} = 31\,\mathrm{yr}$), *J. Phys. G: Nucl. Part. Phys.* **18**, 393 (1992).

[9] O. A. P. Tavares, E. L. Medeiros and M. L. Terranova, Alpha decay half-life of bismuth isotopes, *J. Phys. G: Nucl. Part. Phys.* **31**, 129 (2005).

[10] O. A. P. Tavares and E. L. Medeiros, A simple description of cluster radioactivity, *Phys. Scr.* **86**, 015201 (2012).

[11] O. A. P. Tavares and M. L. Terranova, Toward an accurate determination of half-life of ^{147}Sm isotope, *Appl. Radiat. Isot.* **139**, 26 (2018).

[12] O. A. P. Tavares and M. L. Terranova, Partial alpha-decay half-lives for alpha-emitting Osmium isotopes: accurate determinations by a semi-empirical model, *Appl. Radiat. Isot.* **160**, 109034 (2020).

[13] O. A. P. Tavares, E. L. Medeiros and M. L. Terranova, Alpha-decay half-life of Hafnium isotopes reinvestigated by a semi-empirical approach, *Appl. Radiat. Isot.* **166**, 109381 (2020).

[14] G. Gamow, Zur Quantentheorie des Atomkernes, *Z. Phys.* **51**, 204 (1928).

[15] R. W. Gurney and E. U. Condon, Quantum mechanics and radioactive disintegration, *Nature* **122**, 439 (1928).

[16] R. W. Gurney and E. U. Condon, Quantum mechanics of radioactive disintegration, *Phys. Rev.* **33**, 127 (1929).

[17] P. de Marcillac, N. Coron, G. Dambier, J. Leblanc and J. -P. Moalic, Experimental detection of α-particles from the radioactive decay of natural bismuth, *Nature* **422**, 876 (2003).

[18] P. Möller, J. R. Nix, W. D. Myers and W. J. Swiatecki, Nuclear ground-state masses and deformations, *At. Data Nucl. Data Tables* **59**, 185 (1995).

[19] W. D. Myers, *Droplet Model of Atomic Nuclei* (Plenum: New York, 1977).

[20] P. Möller, A. J. Sierk, T. Ichikawa and H. Sagawa, Nuclear ground-state masses and deformations: FRDM (2012), *At. Data Nucl. Data Tables* **109–110**, 1 (2016).

[21] I. Sick, J. S. McCarthy and R. R. Whitney, Charge density of ^{4}He, *Phys. Lett. B* **64**, 33 (1976).

[22] E. L. Medeiros, M. M. N. Rodrigues, S. B. Duarte and O. A. P. Tavares, Systematics of alpha-decay half-life: new evaluations for alpha-emitter nuclides, *J. Phys. G*: *Nucl. Part. Phys.* **32**, B23 (2006).

[23] M. Wang, G. Audi, F. G. Kondev, W. J. Huang, S. Naimi and X. Xu, The AME2016 atomic mass evaluation (II) Tables, graphs and references, *Chin. Phys. C* **41**, 030003 (2017).

[24] K. -N. Huang, M. Aoyagi, M. H. Chen, B. Crasemann and H. Bart, Neutral-atom electron binding energies from relaxed-orbital relativistic Hartree-Fock-Slater calculations $2 \leq Z \leq 106$, *At. Data Nucl. Data Tables* **18**, 243 (1976).

[25] E. Browne and H. Junde, Nuclear Data Sheets for $A = 174$, *Nucl. Data Sheets* **87**, 15 (1999).

[26] J. Magill, R. Dreher and Zs. Sóti, *Karlsruher Nuklidkarte* 10$^{\text{th}}$ Edition (2018).

[27] V. Caracciolo, S. S. Nagorny, P. Belli, R. Bernabei, F. Cappella, R. Cerulli, A. Incicchitti, M. Laubenstein, V. Merlo, S. Nisi and P. Wang, Search for α decay of naturally occurring Hf-nuclides using a Cs_2HfCl_6 scintillator, *Nucl. Phys. A* **1002**, 121941 (2020).

[28] M. Braun, Y. M. Georgiev, T. Schönherr, H. Wilsenach and K. Zuber, A new precision measurement of the α-decay half-life of ^{190}Pt, *Phys. Lett. B* **768**, 317 (2017).

[29] J. W. Beeman, M. Biassoni, C. Brofferio *et al.*, First Measurement of the Partial Widths of ^{209}Bi Decay to the Ground and to the First Excited States, *Phys. Rev. Lett.* **108**, 062501 (2012).

[30] F. G. Kondev and S. Lalkovski, Nuclear Data Sheets for $A = 207$, *Nucl. Data Sheets* **112**, 707 (2011).

[31] A. A. Voinov, V. K. Utyonkov, Yu. Oganessian *et al.*, Synthesizing and Studying Superheavy Nuclei ^{294}Ts and ^{294}Og, *Bull. Russian Acad. Sci.: Physics* **84**, 351 (2020).

[32] J.-G. Deng, H.-F. Zhang and G. Royer, Improved empirical formula for α-decay half-lives, *Phys. Rev. C* **101**, 034307 (2020).

[33] M. Gonçalves and S. B. Duarte, Effective liquid drop description for the exotic decay of nuclei, *Phys. Rev. C* **48**, 2409 (1993).

[34] X. Zhang and Z. Ren, α-decay half-lives of ground and isomeric states calculated in a unified theoretical framework, *J. Phys. G: Nucl. Part. Phys.* **31**, 959 (2005).

[35] Y. Ren and Z. Ren, New Geiger-Nuttal law for α-decay of heavy nuclei, *Phys. Rev. C* **85**, 044608 (2012).

Table 1 - Anticipating by G_{r}-values [Eq. (25) plus (26)] the most likely modes of α-decay of $^{178}\mathrm{Hf}^{m2}$ isomer ($J^{\pi} = 16^{+}$) to levels of the ground-state band of $^{174}\mathrm{Yb}$. The lower G_{r} the more likely is its corresponding α-transition expected to occur.

Level of $^{174}\mathrm{Yb}$[a]		α-transition		G_{r}-value
E^{*}_{D}(MeV)	J^{π}_{D}	Q_{α}(MeV)[b]	ℓ	(fm·MeV$^{1/2}$)
0	0^{+}	4.55855	16	107.35
0.07647	2^{+}	4.48208	14	101.93
0.253117	4^{+}	4.305433	12	98.91
0.526034	6^{+}	4.032516	10	98.58
0.88993	8^{+}	3.66862	8	101.52
1.3360	10^{+}	3.22255	6	108.67
1.8610	12^{+}	2.69755	4	122.02
2.4570	14^{+}	2.10155	2	145.54

[a] Data taken from [25].

[b] $Q_{\alpha} = 4.55855 - E^{*}_{\mathsf{D}}$ MeV (screening of 0.0281 MeV considered).

Table 2 - Input data for selected α-emitting ground and isomeric states to determine values of parameter g (last column) of the present heavy-particle decay calculation model.[a]

Alpha-decay case	Q_α(MeV)[b]	J^π_{P}	J^π_{D}	ℓ[c]	$T^{\mathrm{t}}_{1/2}$	b_α (%)	g[e]
${}^{151}_{63}\mathrm{Eu} \to {}^{147}_{61}\mathrm{Pm}$	1.9874	$5/2^+$	$7/2^+$	2	4.6×10^{18} yr	100	0.267
${}^{151}_{67}\mathrm{Ho}^m \to {}^{147}_{65}\mathrm{Tb}$	4.7611	$1/2^+$	$1/2^+$	0	47.2 s	77	0.142
${}^{152}_{67}\mathrm{Ho}^m \to {}^{148}_{65}\mathrm{Tb}^m$	4.6025	9^+	9^+	0	49.8 s	10.8	0.155
${}^{153}_{67}\mathrm{Ho}^m \to {}^{149}_{65}\mathrm{Tb}$	4.1455	$1/2^+$	$1/2^+$	0	9.3 min	0.18	0.185
${}^{155}_{71}\mathrm{Lu} \to {}^{151}_{69}\mathrm{Tm}$	5.8303	$11/2^-$	$11/2^-$	0	68.6 ms	90	0.135
${}^{156}_{71}\mathrm{Lu} \to {}^{152}_{69}\mathrm{Tm}$	5.6233	2^-	2^-	0	494 ms	95	0.136
${}^{157}_{71}\mathrm{Lu}^m \to {}^{153}_{69}\mathrm{Tm}$	5.1563	$11/2^-$	$11/2^-$	0	4.79 s	6	0.153
${}^{157}_{73}\mathrm{Ta}^m \to {}^{153}_{71}\mathrm{Lu}$	6.4053	$11/2^-$	$11/2^-$	0	4.3 ms	99	0.141
${}^{180}_{74}\mathrm{W} \to {}^{176}_{72}\mathrm{Hf}$	2.5446	0^+	0^+	0	1.8×10^{18} yr	100	0.196
${}^{186}_{76}\mathrm{Os} \to {}^{182}_{74}\mathrm{W}$	2.8518	0^+	0^+	0	2.0×10^{15} yr	100	0.157
${}^{209}_{83}\mathrm{Bi} \to {}^{205}_{81}\mathrm{Tl}$	3.1723	$9/2^-$	$1/2^+$	5	2.01×10^{19} yr	98.8	0.447
${}^{211}_{84}\mathrm{Po}^m \to {}^{207}_{82}\mathrm{Pb}^m$	7.4588	$25/2^+$	$13/2^+$	6	25.2 s	91	0.497
${}^{211}_{84}\mathrm{Po}^m \to {}^{207}_{82}\mathrm{Pb}$	9.0922	$25/2^+$	$1/2^-$	13	25.2 s	7.04	0.586
${}^{212}_{84}\mathrm{Po}^m \to {}^{208}_{82}\mathrm{Pb}$	11.9128	18^+	0^+	18	45.1 s	97	0.576
${}^{213}_{88}\mathrm{Ra}^m \to {}^{209}_{86}\mathrm{Rn}$	8.6680	$17/2^-$	$5/2^-$	6	2.2 ms	0.41	0.567
${}^{217}_{89}\mathrm{Ac}^m \to {}^{213}_{87}\mathrm{Fr}^m$	10.2921	$29/2^+$	$21/2^-$	5	740 ns	3.87	0.509
${}^{218}_{92}\mathrm{U}^m \to {}^{214}_{90}\mathrm{Th}$	10.9248	8^+	0^+	8	560 μs	100	0.560
${}^{235}_{92}\mathrm{U} \to {}^{231}_{90}\mathrm{Th}$	4.5137	$7/2^-$	$7/2^-$	0	7.04×10^{8} yr	57.73	0.196
${}^{235}_{92}\mathrm{U} \to {}^{231}_{90}\mathrm{Th}$	4.4821	$7/2^-$	$9/2^-$	2	7.04×10^{8} yr	18.92	0.196
${}^{237}_{93}\mathrm{Np} \to {}^{233}_{91}\mathrm{Pa}$	4.9125	$5/2^+$	$5/2^+$	0	2.144×10^{6} yr	47.64	0.190
${}^{237}_{93}\mathrm{Np} \to {}^{233}_{91}\mathrm{Pa}$	4.8953	$5/2^+$	$7/2^+$	2	2.144×10^{6} yr	23.2	0.184
${}^{237}_{93}\mathrm{Np} \to {}^{233}_{91}\mathrm{Pa}$	4.7611	$5/2^+$	$5/2^+$	0	2.144×10^{6} yr	6.42	0.155
${}^{239}_{94}\mathrm{Pu} \to {}^{235}_{92}\mathrm{U}$	5.2867	$1/2^+$	$1/2^+$	0	2.411×10^{4} yr	70.77	0.163
${}^{239}_{94}\mathrm{Pu} \to {}^{235}_{92}\mathrm{U}$	5.2738	$1/2^+$	$3/2^+$	2	2.411×10^{4} yr	17.11	0.214
${}^{239}_{94}\mathrm{Pu} \to {}^{235}_{92}\mathrm{U}$	5.2351	$1/2^+$	$5/2^+$	2	2.411×10^{4} yr	11.94	0.199
${}^{247}_{96}\mathrm{Cm} \to {}^{243}_{94}\mathrm{Pu}$	4.9947	$9/2^-$	$9/2^-$	0	1.56×10^{7} yr	71	0.147
${}^{247}_{96}\mathrm{Cm} \to {}^{243}_{94}\mathrm{Pu}$	4.9423	$9/2^-$	$11/2^-$	2	1.56×10^{7} yr	4.7	0.244
${}^{251}_{98}\mathrm{Cf} \to {}^{247}_{96}\mathrm{Cm}$	6.2221	$1/2^+$	$9/2^-$	5	900 yr	2.6	0.552
${}^{251}_{98}\mathrm{Cf} \to {}^{247}_{96}\mathrm{Cm}$	6.1604	$1/2^+$	$11/2^-$	5	900 yr	12.5	0.387

[a] J^π_i-values [i = P (parent nucleus), D (daughter product nucleus)] are those reported in [4]; total half-life values, $T^{\mathrm{t}}_{1/2}$, were taken from [4, 26]; total α-branching values, b_α, were computed from data available in most recent Nuclear Data Sheets publications or in [4].

[b] Screening effect due to surrounding electrons taken into account [eq. (13)].

[c] This is the minimum, mutual angular momentum associated with the rotation of the producing nuclei around their common centre of mass.

Table 3 - Partial α-decay half-lives of $^{178}Hf^{m2}$ isomer to levels of the ground-state-band of ^{174}Yb isotope according to the present calculation model.[a]

Level of ^{174}Yb[b]		alpha transition			α-half-life and Intensity	
E^*_D(MeV)	J^π	ℓ	Q_α(MeV)[c]	g^c-value[d]	$T^c_{1/2}$(Gyr)[e]	I_α(%)
0	0^+	16	4.55855	0.585	$(1.5 \pm 0.7) \times 10^3$	~ 0
0.07647	2^+	14	4.48208	0.578	11 ± 5	~ 2.2
0.253117	4^+	12	4.305433	0.570	0.68 ± 0.30	~ 36
0.526034	6^+	10	4.032516	0.560	0.43 ± 0.18	~ 57
0.88993	8^+	8	3.66862	0.555	5.2 ± 2.1	~ 4.7
1.3360	10^+	6	3.22255	0.525	$(1.7 \pm 0.7) \times 10^3$	~ 0
1.8610	12^+	4	2.69755	0.400	$(3.8 \pm 1.4) \times 10^7$	~ 0
2.4570	14^+	2	2.10155	0.217	$(2.8 \pm 1.0) \times 10^{15}$	~ 0

[a] $^{178}Hf^{m2}$ isomer: $T^t_{1/2} = 31$ yr; $J^\pi = 16^+$; $E^*_P = 2.44609$ MeV; measured total alpha-decay half-life, $T^\alpha_{1/2} = (25 \pm 5)$ Gyr [7].

[b] Data taken from [25].

[c] $Q_\alpha = 4.55855 - E^*_D$ (MeV); screening of 0.0281 MeV considered.

[d] Estimated values from curve of Fig. 2.

[e] Calculated total alpha-decay half-life, $T^{ct\alpha}_{1/2} = (0.24 \pm 0.07)$ Gyr.

Table 4 - Comparison between experimental and calculated partial α-decay half-life values for some selected α-transitions.

Decay case	Q_α (MeV)[a]	ℓ	g-value	Alpha-decay half-life, $T^{\alpha}_{1/2}$		
				Calculated[b]	Experimental	Ref.
^{147}Sm $\to$ ^{143}Nd	2.33327	0	0.093 [c]	$(1.3 \pm 0.6) \times 10^{11}$ yr	$(1.063 \pm 0.005) \times 10^{11}$ yr	[11]
^{151}Eu $\to$ ^{147}Pm	1.98735	2	0.217	$(2.9 \pm 1.4) \times 10^{18}$ yr	$(4.6 \pm 1.2) \times 10^{18}$ yr	[4]
^{152}Gd $\to$ ^{148}Sm	2.22786	0	0.161	$(4.5 \pm 2.1) \times 10^{14}$ yr	$(1.08 \pm 0.08) \times 10^{14}$ yr	[4]
^{174}Hf $\to$ ^{170}Yb	2.52262	0	0.161	$(5.9 \pm 2.8) \times 10^{16}$ yr	$(7.0 \pm 1.2) \times 10^{16}$ yr	[27]
^{180}W $\to$ ^{176}Hf	2.54460	0	0.161	$(1.1 \pm 0.5) \times 10^{18}$ yr	$(1.8 \pm 0.2) \times 10^{18}$ yr	[4]
^{186}Os $\to$ ^{182}W	2.85182	0	0.103 [d]	$(1.0 \pm 0.5) \times 10^{15}$ yr	$(2.0 \pm 1.1) \times 10^{15}$ yr	[12]
^{190}Pt $\to$ ^{186}Os	3.30036	0	0.161	$(2.7 \pm 1.2) \times 10^{11}$ yr	$(4.97 \pm 0.16) \times 10^{11}$ yr	[28]
^{177}Tl^m $\to$ ^{173}Au^m	7.69369	0	0.161	(309 ± 98) μs	367 ± 122 μs	[4]
^{209}Bi $\to$ ^{205}Tl	3.17227	5	0.474	$(2.6 \pm 1.3) \times 10^{19}$ yr	$(2.04 \pm 0.08) \times 10^{19}$ yr	[29]
^{211}Po^m $\to$ ^{207}Pb	9.09219	13	0.586	(5.1 ± 1.7) min	(5.97 ± 0.14) min	[30]
^{212}Po^m $\to$ ^{208}Pb	11.91282	18	0.570	(44 ± 15) s	(45.13 ± 0.06) s	[4]
^{202}At^m $\to$ ^{198}Bi^m	6.30012	0	0.161	(0.15 ± 0.05) h	(0.58 ± 0.01) h	[4]
^{253}Lr^m $\to$ ^{249}Md^m	8.89682	0	0.161	(0.91 ± 0.30) s	(1.47 ± 0.15) s	[4]
^{293}Ts $\to$ ^{289}Mc	11.35333	2	0.217	(10 ± 3) ms	22 ms	[31]
^{294}Og $\to$ ^{290}Lv	11.90011	0	0.161	(0.34 ± 0.11) ms	0.69 ms	[31]

[a] Values obtained by eqs. (12) and (13), with $\Delta M'$s taken from [23].

[b] This work, eqs. (33)–(35).

[c] Quoted in [11].

[d] Quoted in [12].

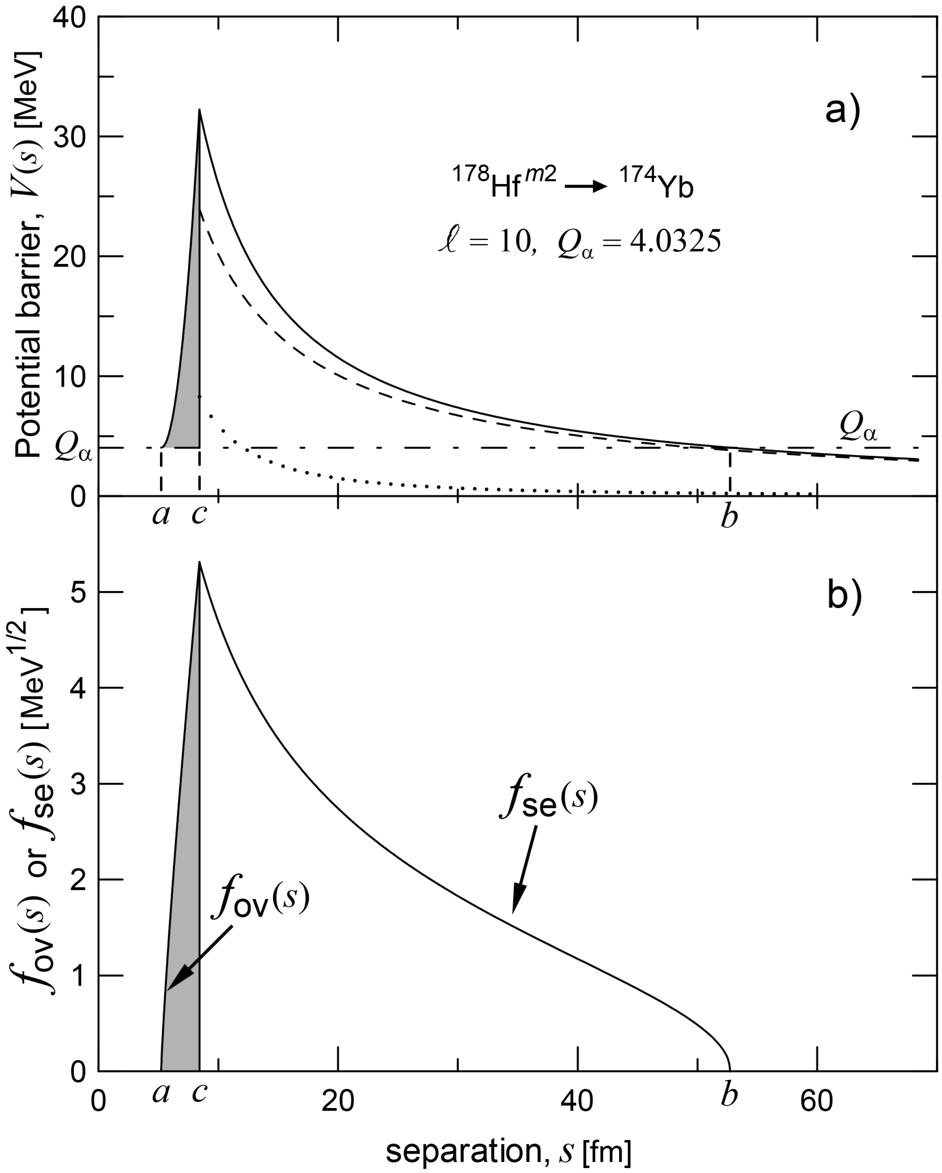

Fig. 1 Part (a): Potential barrier for α-decay of ^{178}Hf^{m2} isomer ($J^\pi = 16^+$) to the level of excitation at 0.526 MeV, $J^\pi = 6^+$, of ^{174}Yb. Dotted line indicates the centrifugal barrier; short-dashed line the Coulomb barrier; full line the total potential barrier. The long dash-dotted line indicates the Q_α-value of the decay process. The overlapping region a–c is emphasized by the shaded area, and the separation region is defined in the interval c–b. Part (b): The corresponding functions $f_i(s) = [V(s) - Q_\alpha]^{1/2}$ [i = ov (overlapping region), se (separation region)] to calculate the WKB-integrals that give the reduced Gamow factor, G_r (eq. (20)).

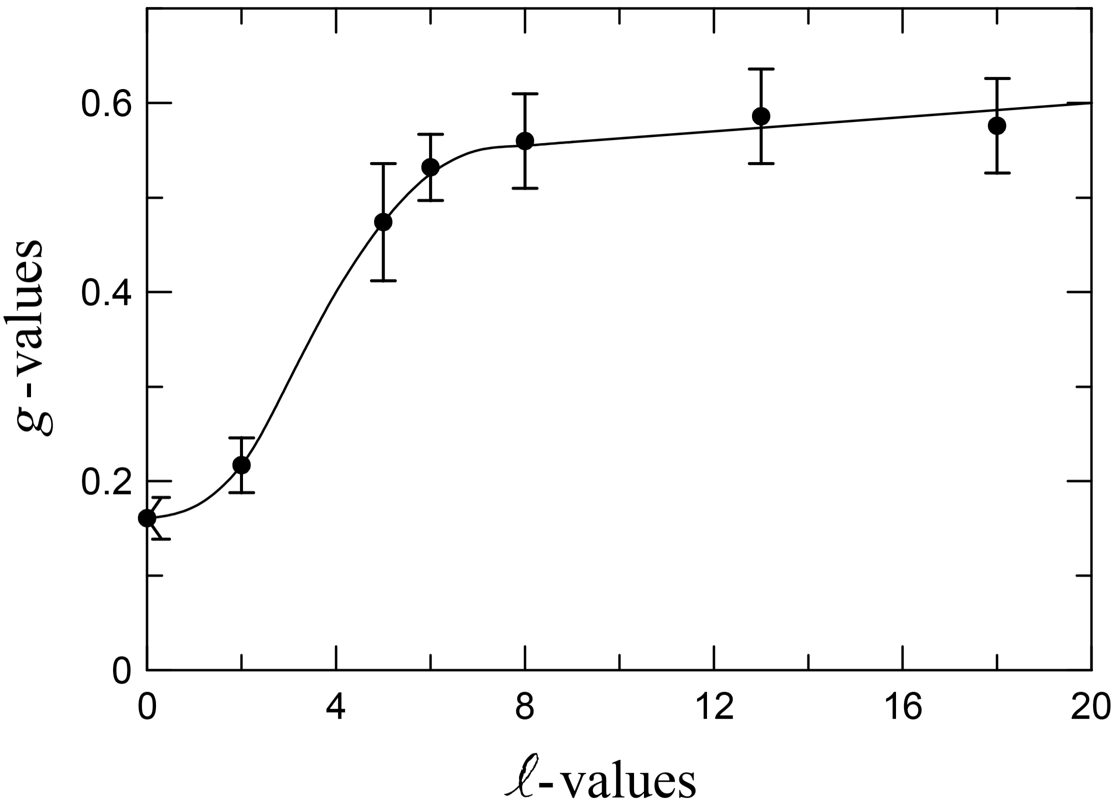

Fig. 2 Showing the correlation between parameter g and angular momentum ℓ. Points represent average semi-empirical $g^{\rm e}$-values listed in Table 2 (last column) (for $\ell = 8$, 13, and 18 there is only one $g^{\rm e}$-value). The curve is an eye-fit through the points.

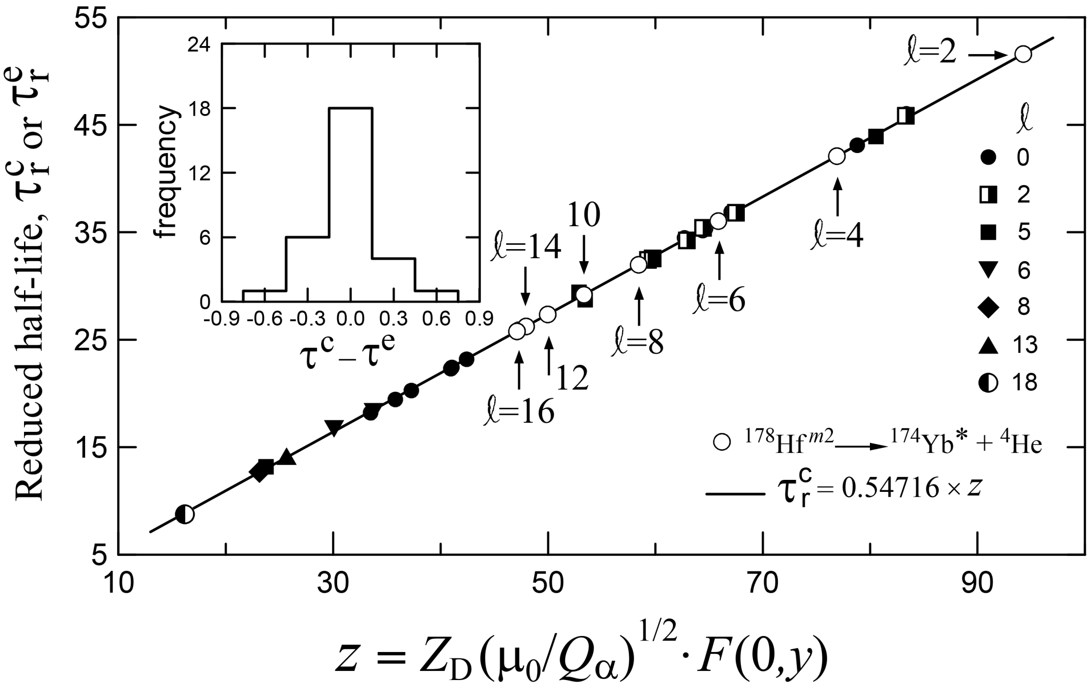

Fig. 3 Reduced half-life, $\tau_{\mathsf{r}} = \tau_{\mathsf{coul}}$ (Eq. (28)), plotted against the quantity z. The line $\tau_{\mathsf{r}}^{\mathsf{c}} = 0.54716{\cdot}z$ represents the location of calculated $\tau_{\mathsf{r}}^{\mathsf{c}}$-values. The darkened points are experimental $\tau_{\mathsf{r}}^{\mathsf{e}}$-values (obtained by (30)) for the twenty-nine cases of α-decay listed in Table 2 (grouped by ℓ) that have been used to obtain the dependence g *vs* ℓ. Open circles correspond to $\tau_{\mathsf{r}}^{\mathsf{c}}$-values for α-decay of ^{178}Hf^{m2} isomer to eight levels in the ground-state band of ^{174}Yb (ℓ-values are indicated near the points). The distribution of $\tau_{\mathsf{r}}^{\mathsf{c}} - \tau_{\mathsf{r}}^{\mathsf{e}} = \tau^{\mathsf{c}} - \tau^{\mathsf{e}}$ is depicted in the inset graph (in 93 % of cases τ^{c} differs from τ^{e} by only 33 % on the average).

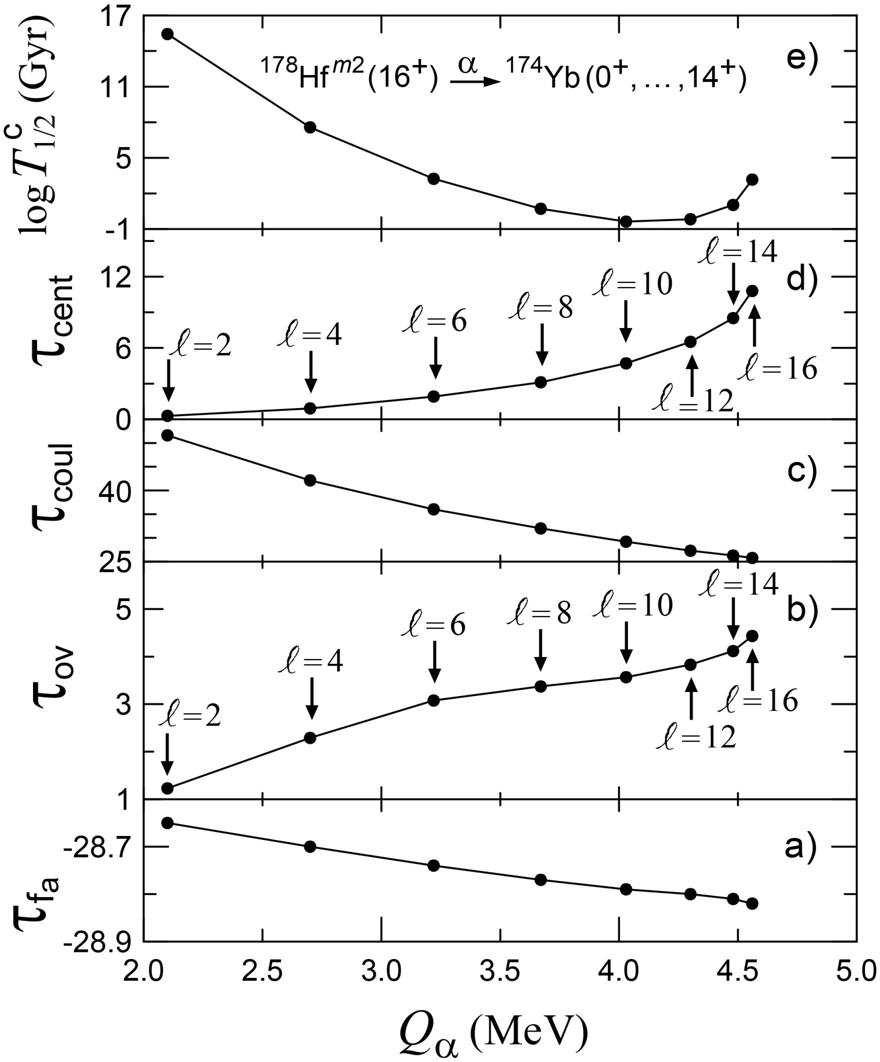

Fig. 4 Showing the contributions to partial half-life, $T^{\alpha}_{1/2}$, for α-transitions of ^{178}Hf^{m2} ($J^{\pi} = 16^{+}$) isomer to different levels of ^{174}Yb ($J^{\pi} = 0^{+}, 2^{+}, \ldots, 14^{+}$): frequency of assaults to the barrier, τ_{fa} (a); overlapping region, τ_{ov} (b); Coulomb separation region, τ_{coul} (c); and centrifugal contribution, τ_{cent} (d). Part (e) displays the values of $\tau = \tau_{\mathsf{fa}} + \tau_{\mathsf{ov}} + \tau_{\mathsf{coul}} + \tau_{\mathsf{cent}} = \log_{10} T^{\alpha}_{1/2}$ (Gyr). Points joined by lines represent calculated values of this work. Minimum angular momentum, ℓ, used in τ_{ov} and τ_{cent} is indicated. It is seen a clear minimum of $T^{\alpha}_{1/2}$ at $Q_{\alpha} \approx 4.03\,$MeV, $\ell = 10$.

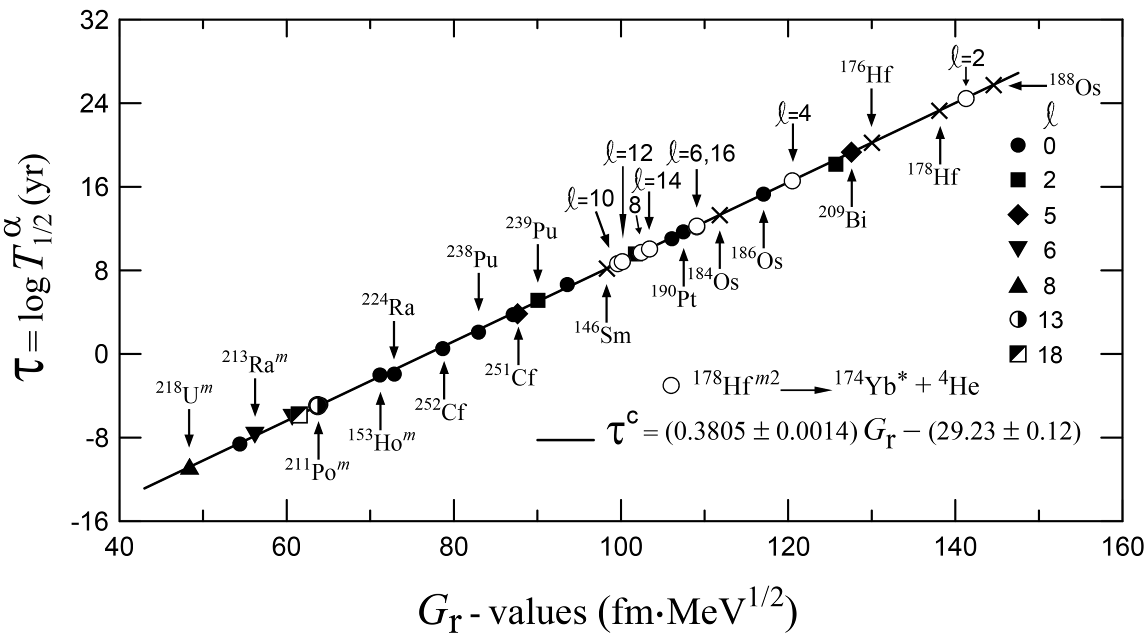

Fig. 5 Dependence of α-decay half-life, τ, upon reduced Gamow factor, $G_{\mathsf{r}} = G_{\mathsf{r}}^{\mathsf{ov}} + G_{\mathsf{r}}^{\mathsf{se}}$. The twenty darkened points represent measured values taken from the literature. G_{r} is calculated from (34) if $\ell = 0$, or from (33) if $\ell \neq 0$. Open circles are calculated values of the eight cases for $^{178}\mathrm{Hf}^{m2} \to \mathrm{Yb}\,(\ell = 2, 4, \ldots, 16)$ decays, and crosses locate some of the calculated data listed in Table 4. A number of parent emitter nuclides are indicated by arrows, and the line is the linear least-squares fit to experimental data.

NOTAS DE FÍSICA é uma pré-publicação de trabalho original em Física.
Pedidos de cópias desta publicação devem ser enviados aos autores ou ao:

Centro Brasileiro de Pesquisas Físicas
Área de Publicações
Rua Dr. Xavier Sigaud, 150 – 4º andar
22290-180 – Rio de Janeiro, RJ
Brasil
E-mail: alinecd@cbpf.br/valeria@cbpf.br
http://portal.cbpf.br/publicacoes-do-cbpf

NOTAS DE FÍSICA is a preprint of original unpublished works in Physics.
Requests for copies of these reports should be addressed to:

Centro Brasileiro de Pesquisas Físicas
Área de Publicações
Rua Dr. Xavier Sigaud, 150 – 4º andar
22290-180 – Rio de Janeiro, RJ
Brazil
E-mail: alinecd@cbpf.br/valeria@cbpf.br
http://portal.cbpf.br/publicacoes-do-cbpf